Diffractive vector and scalar integrals for bistatic radio holographic remote sensing

A. G. Pavelyev

Institute of Radio Engineering and Electronics, Russian Academy of Sciences, Moscow, Russia

Y. A. Liou

Centre for Space and Remote Sensing Research, National Central University, Jung-Li, Taiwan

J. Wickert

GeoForschungsZentrum Potsdam, Potsdam, Germany

Received 10 July 2003; revised 9 May 2004; accepted 26 May 2004; published 26 August 2004.

[1] We introduce new vector diffractive integrals, which can be used for the radio holographic remote sensing of the atmosphere and terrestrial surfaces. These integrals are exact relationships connecting the electromagnetic fields known at some interface or curve in space with radio fields on the terrestrial surface or inside the atmosphere. They allow one to restore the radio image of the atmosphere or Earth surface in the investigated regions using a radio hologram registered in space by a small instrument installed on the low Earth orbit satellite. The high-precision radio signals of the Global Positioning System (GPS) navigational satellites can be used as a source of the radio emission for radio holograms. We indicated a connection between the vector diffractive integrals and scalar diffractive integral, which is now applied for the GPS occultation investigation of Earth's atmosphere under an assumption of the spherical symmetry. For the atmosphere itself the accuracy of the scalar theory corresponds to the accuracy of the GPS occultation measurements. The most significant factor that affects the polarization is the reflection from the surface. The use of vector theory can thus be useful for the investigation of Earth's atmosphere by detecting the reflected rays. We show that the reference signal needed for restoration of the radio field from the registered radio hologram is coinciding with the Green function of the scalar wave equation corresponding to a three-dimensional inhomogeneous medium. This substantiates the radio holographic–focused synthetic aperture principle (RFSA) in its application to the atmosphere and surface research. We validated the high vertical resolution of the RFSA method by obtaining radio image of the atmosphere and Earth's surface. Zverev's diffractive integral is used to compare the canonical transform (CT), back propagation (BP), and RFSA methods. For comparison, a general inverse operator (GIO) is introduced. The CT and BP transforms can be obtained by application of the GIO transform to Zverev's diffractive integral. The CT method can resolve physical rays in multipath situations under an assumption of the global spherical symmetry of the atmosphere and ionosphere. The RFSA method can account for the multipath in the case when the global spherical symmetry is absent by using the appropriate model of the refractivity and has a promise to be effective for operational data analysis. *INDEX TERMS:* 6904 Radio Science: Atmospheric propagation; 6909 Radio Science: Electromagnetic metrology; 6964 Radio Science: Radio wave propagation; 6969 Radio Science: Remote sensing; *KEYWORDS:* remote sensing, radio wave propagation, atmospheric propagation

0048-6604/04/2003RS002935$11.00

Citation: Pavelyev, A. G., Y. A. Liou, and J. Wickert (2004), Diffractive vector and scalar integrals for bistatic radio holographic remote sensing, *Radio Sci.*, *39*, RS4011, doi:10.1029/2003RS002935.

1. Introduction

[2] The method of the wave front inversion consists of determining the radio field inside the inhomogeneous media using a radio hologram registered on some interface or curve in space. The name of the method has been introduced by *Zeldovich et al.* [1985]. They described its application for the optical sounding of the inhomogeneous media. Unlike the optical range, the digital methods are applied for the radio holographic remote sensing. The digital methods for remote sensing use the diffractive integrals connecting the electromagnetic fields on some interface or curve in the space (e.g., the orbital trajectory of a low Earth orbit (LEO) satellite with a radio holographic receiver) with the field in the space between the transmitter and receiver. *Zverev* [1975] obtained the three-dimensional (3-D) scalar equation, which links the angular spectrum of the field with the angular spectrum of the back-propagated wave in the free space. *Marouf and Tyler* [1982] described the inversion method for obtaining the spatial structure of Saturn's rings using the radio holograms registered onboard Voyager spacecraft. They constructed a reference signal using the known form of the rings and diffraction theory and obtained spatial resolution about of 1/10–1/100 of the Fresnel's zone size. *Kunitsyn and Tereshchenko* [1991] and *Kunitsyn et al.* [1994] considered the application of the tomographic method for the remote sensing of Earth's ionosphere using the radio emission of the LEO satellites. *Gorbunov et al.* [1996] introduced the back-propagation (BP) method on the basis of the scalar diffractive 2-D integral, to heighten the vertical resolution in the radio occultation (RO) experiments. The BP method has a significant difference in comparison with the radio holographic approach suggested by *Marouf and Tyler* [1982]. Back propagation is performed using the 2-D free space Green function rather than the Green function obtained as a solution of a boundary diffraction problem in a 3-D medium. *Pavelyev* [1998], *Hocke et al.* [1999], and *Igarashi et al.* [2000, 2001] derived a radio holographic–focused synthetic aperture (RFSA) principle for RO data analysis. The Fourier analysis in the finite time intervals is applied to the product of the RO and reference signals with the aims (1) to obtain 1-D radio images of the atmosphere and terrestrial surface and (2) to retrieve the vertical profiles of the physical parameters in the atmosphere and mesosphere. Using their method, one can directly determine the dependence of the refraction angle on the impact parameter without application of complex BP technology. *Hocke et al.* [1999] and *Igarashi et al.* [2000, 2001] determined by the RFSA method the electron density $N_e(h)$ and its vertical gradient $dN_e(h)/dh$ in the mesosphere and temperature $T(h)$ in the atmosphere. *Beyerle and Hocke* [2001] and *Igarashi et al.* [2001] applied the RFSA method to visualize signals reflected from the terrestrial surface. They were the first to reveal surface reflections and obtained 1-D radio images of the troposphere and the surface by analyzing the Global Positioning System/Meteorology Experiment (GPS/MET) RO data. *Igarashi et al.* [2001] and *Pavelyev et al.* [2002a] provided preliminary analysis of radio images and estimated the vertical resolution of the RFSA method as about of 70 m. *Beyerle et al.* [2002] applied the RFSA method for a radio holographic analysis of the GPS signal propagation in the troposphere and surface reflections. They obtained important information on a global scale on the humidity concentration in the boundary layer of the atmosphere using the CHAMP RO data. It may be noted that the RFSA method is distinctive in comparison with the unfocused synthetic aperture (Doppler selection) method applied early by *Lindal et al.* [1987] for the spectral analysis of the RO data to obtain the radio images of Uranus' atmosphere. *Gorbunov* [2002a, 2002b] used also the representation of the wave field as a sum of spherical waves to correct approximately for the wave front curvature and considered examples of radio images with multiple direct and reflected rays for the GPS/MET RO data. In the case of unfocused synthesis, the size of the synthetic aperture and the vertical resolution are limited by an uncertainty condition between resolution in the impact parameter and refraction angle [*Gorbunov et al.*, 2000]. The RFSA method, in principle, does not obey the uncertainty condition because it accounts for the curvature of the wave fronts corresponding to the physical rays after propagation in Earth's atmosphere and can use the large size of the synthetic aperture for effective compression of the angular plane wave spectrum of the RO signal. According to this advantage, the RFSA method can discern the surface reflections near the powerful tropospheric RO signal and can realize in practice the high values of the vertical resolution $\sim$100 m as expected early for the BP method [*Hocke et al.*, 1999; *Igarashi et al.*, 2000, 2001]. Note, however, that to achieve high resolution in the multipath areas, one must use an accurate model of the refractivity in the RO region to construct the reference signal, which has high level of coherence with the RO signal. Recently, *Gorbunov* [2002c] introduced the canonical transform (CT) method for processing the GPS RO data in lower troposphere. The main idea of the CT method consists of using Fourier integral operators (FIO) to find directly the dependence of the refraction angle on the impact parameter for each physical ray in multipath conditions. *Jensen et al.* [2003] introduced the full spectrum inversion (FSI) method to process the RO signals.

They established a novel connection between the derivative of the phase of a physical ray on the instantaneous frequency in the full Fourier spectrum of the RO signal and the time of intersection of the physical ray with orbital trajectory of LEO satellite. This feature of the FSI method can be used to obtain under an assumption of spherical symmetry the refraction angle and impact parameter for each physical ray.

[3] The progress in developing the radio holographic investigations is connected, in particular, with existence of the radio navigational satellite systems GPS/Global Navigation Satellite System (GLONASS), which are emitting high-precision, coherent, and stable radio signals. The diffractive integrals can be used to realize the high precision and stability of the radio signals of the radio navigational systems and to obtain extreme values of the spatial resolution and accuracy in the remote sensing of the atmosphere and surface of Earth from space. The aim of this paper consists of the presentation of the diffractive vector integrals for bistatic radio holographic remote sensing of the terrestrial surface and atmosphere, substantiating the RFSA method, introducing a simple way to obtain the CT and BP transforms and establishing their limitations using a GIO. In section 2 we derive the diffractive 3-D vector integrals for describing the direct propagation of the radio waves in the 3-D inhomogeneous media. To accomplish this end, we modernize the Stratton-Chu vector theory developed early for the case of 3-D homogeneous media [*Stratton*, 1941]. The derived vector equations include Green function, which is a solution of the 3-D scalar wave equation for an inhomogeneous medium. This is significantly different from results obtained early by *Müller* [1969] and *Ström* [1991] for an inhomogeneous medium because their vector equations contain the free space Green function. In section 3 we derive 3-D vector equations for back-propagating radio waves and then show that the scalar 2-D diffractive integral can be derived from the 3-D vector diffractive integrals for a 2-D medium. A connection between the solution of 3-D diffraction problem and the reference signal for the RFSA method is established in section 4. In section 4 we derived the basic equations of the RFSA method, illustrated its capability to compress the angular spectrum of the RO signal, and achieved high vertical resolution. In section 5 we compared the RFSA, CT, and BP methods and established their limitations using the GIO transform.

2. Vector Equations for Radio Fields in the 3-D Inhomogeneous Medium (Direct Propagation)

[4] The problem of expressing the electric and magnetic vectors $\boldsymbol{E}$, $\boldsymbol{H}$ of the radio field at an interior point in terms of the values $\boldsymbol{E}$, $\boldsymbol{H}$ over an enclosing surface S (Figure 1) has been considered for the homogeneous medium by *Stratton* [1941]. Radio holographic equations for 3-D inhomogeneous medium may be obtained by applying a vector analogue of Green's theorem to the field equations. It was shown that if $\boldsymbol{P}$ and $\boldsymbol{Q}$ are two vector functions of position with the proper continuity, then

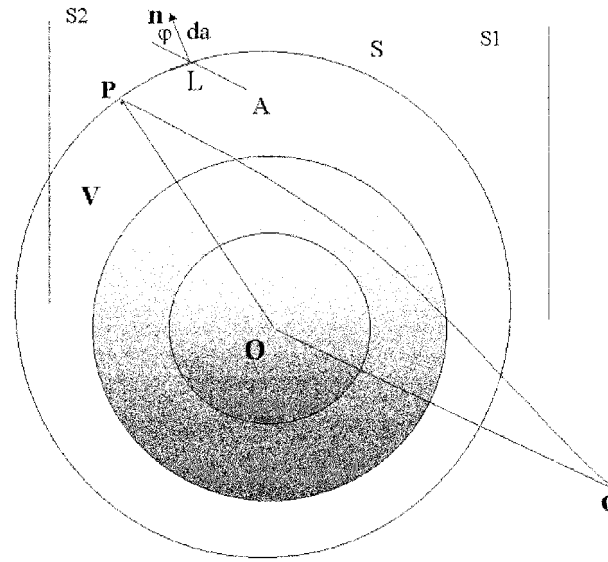

Figure 1. The inhomogeneous volume V and its boundary S.

$$\int_v (\boldsymbol{Q}\nabla \times \nabla \times \boldsymbol{P} - \boldsymbol{P}\nabla \times \nabla \times \boldsymbol{Q})\boldsymbol{dv} = \int_s (\boldsymbol{P} \times \nabla \times \boldsymbol{Q} - \boldsymbol{Q} \times \nabla \times \boldsymbol{P})\boldsymbol{n}\, da, \quad (1)$$

where S is a regular surface (Figure 1) bounding the volume V, and $\boldsymbol{n}$ is the normal to the surface S oriented in the outward direction relative to volume V [*Stratton*, 1941, section 4.14]. The field vectors contain the time only as a factor $\exp(-i\omega t)$. The Maxwell's field equations may be written in the form [*Miller and Suvorov*, 1992]:

$$\nabla \times \boldsymbol{E} - i\omega\mu/c\, \boldsymbol{H} = -4\pi/c\, \boldsymbol{J}^*, \qquad \nabla \boldsymbol{H} = 4\pi/\mu\rho^* - \boldsymbol{H}\nabla(ln\mu), \quad (2)$$

$$\nabla \times \boldsymbol{H} + i\omega\varepsilon/c\, \boldsymbol{E} = 4\pi/c\, \boldsymbol{J}, \qquad \nabla \boldsymbol{E} = 4\pi\varepsilon^{-1}\rho - \boldsymbol{E}\nabla(ln\varepsilon), \quad (3)$$

where ε is the electric permittivity, μ is the magnetic permeability of the medium, $\boldsymbol{E}$, $\boldsymbol{H}$ are the electric and magnetic fields, $\boldsymbol{J}$, $\boldsymbol{J}^*$ are the electric and magnetic

currents, and ρ, ρ^* are the electric and magnetic charges. Currents and charges of both types are related by the equations of continuity [*Stratton*, 1941]:

$$\nabla \cdot \boldsymbol{J} - i\omega\rho = 0, \quad \nabla \cdot \boldsymbol{J}^* - i\omega\rho^* = 0. \tag{4}$$

The vectors $\boldsymbol{E}$ and $\boldsymbol{H}$ satisfy

$$\begin{aligned}\nabla \times \nabla \times \boldsymbol{E} - k^2\boldsymbol{E} = {} & i\omega\mu/c(4\pi/c\boldsymbol{J} + [\nabla(ln\mu) \times \boldsymbol{H}]) \\ & - 4\pi/c\nabla \times \boldsymbol{J}^* \\ \nabla \times \nabla \times \boldsymbol{H} - k^2\boldsymbol{H} = {} & i\omega\varepsilon/c(4\pi/c\ \boldsymbol{J}^* - [\nabla(ln\varepsilon) \times \boldsymbol{E}]) \\ & + 4\pi/c\ \nabla \times \boldsymbol{J}\end{aligned}$$

$$k^2 = \omega^2\varepsilon\mu/c^2. \tag{5}$$

[5] According to the method described by *Stratton* [1941], let in equation (1) $\boldsymbol{P} = \boldsymbol{E}$, $\boldsymbol{Q} = \phi\boldsymbol{a}$, where $\boldsymbol{a}$ is a unit vector in an arbitrary direction. The function ϕ (Green's function) is supposed to be a solution of the wave equation:

$$\Delta\phi + k^2\phi = -4\pi\delta(\boldsymbol{r} - \boldsymbol{r}'), \tag{6}$$

where $\delta(\boldsymbol{r} - \boldsymbol{r}')$ is the delta function and $\boldsymbol{r}$, $\boldsymbol{r}'$ are vectors describing the positions of the element of integration at (x, y, z) and the point of observation A at (x', y', z') inside volume V. Distance $|\boldsymbol{r} - \boldsymbol{r}'| = r$ is measured from the element at (x, y, z) to the point of observation at A:

$$r = \left[(x - x')^2 + (y - y')^2 + (z - z')^2\right]^{1/2}. \tag{7}$$

The next relationships can be obtained by using the vector derivative formulas [*Stratton*, 1941] and equation (5) under an assumption that ϕ is a solution of the wave equation (6)

$$\begin{aligned}&\nabla \times \boldsymbol{Q} = \nabla\phi \times \boldsymbol{a}, \nabla \times \nabla \times \boldsymbol{Q} = \boldsymbol{a}k^2\phi + \nabla(\boldsymbol{a} \cdot \nabla\phi), \\ &\nabla \times \nabla \times \boldsymbol{P} = k^2\boldsymbol{E} + i\omega\mu/c(4\pi/c\boldsymbol{J} + [\nabla(ln\mu) \times \boldsymbol{H}]) \\ &\qquad - 4\pi/c\nabla \times J^*, \\ &\boldsymbol{E}\nabla(\boldsymbol{a}\nabla\phi) = \nabla(\boldsymbol{E}(\boldsymbol{a}\nabla a\phi)) - (\boldsymbol{a}\nabla\phi)\nabla(\boldsymbol{E}).\end{aligned} \tag{8}$$

It follows from equations (1)–(8) that

$$\begin{aligned}\int_v & \left(\phi\boldsymbol{a}\left(k^2\boldsymbol{E} + i\omega\mu/c(4\pi/c\boldsymbol{J} + [\nabla(ln\mu) \times \boldsymbol{H}])\right.\right. \\ & \left.\left. - 4\pi/c\nabla \times \boldsymbol{J}^*\right) - \boldsymbol{E}\left(\boldsymbol{a}k^2\phi + \nabla(\boldsymbol{a}\nabla\phi)\right)\right)dv \\ = {} & \int_s (\boldsymbol{E} \times (\nabla\phi) \times \boldsymbol{a} - \phi\boldsymbol{a} \times (i\omega\mu/c\ \boldsymbol{H} - 4\pi/c\boldsymbol{J}^*)) \\ & \boldsymbol{n}\ da.\end{aligned} \tag{9}$$

Using the equation (8), it may be found from equation (9) that

$$\begin{aligned}\int_v & \left(i\omega\mu/c\phi\boldsymbol{a}(4\pi/c\boldsymbol{J} + [\nabla(ln\mu) \times \boldsymbol{H}]) - 4\pi/c\phi\right. \\ & \left.\boldsymbol{a}\nabla \times \boldsymbol{J}^* - \nabla(\boldsymbol{E}(\boldsymbol{a}\nabla\phi)) + (\boldsymbol{a}\nabla\phi)\nabla\boldsymbol{E}\right)dv \\ = {} & \int_s \left([\boldsymbol{E} \times [(\nabla\phi) \times \boldsymbol{a}]] - \phi\boldsymbol{a}\right. \\ & \left.\times (i\omega\mu/c\boldsymbol{H} - 4\pi/c\boldsymbol{J}^*)\right)\boldsymbol{n}da.\end{aligned} \tag{10}$$

One can obtain using the divergence theorem from equation (10)

$$\begin{aligned}\int_v & \left(i\omega\mu/c\phi\boldsymbol{a}(4\pi/c\boldsymbol{J} + [\nabla(ln\mu) \times \boldsymbol{H}])\right. \\ & \left. - 4\pi/c\phi\boldsymbol{a}\nabla \times \boldsymbol{J}^*) + (\boldsymbol{a}\nabla\phi)\nabla\boldsymbol{E}\right)dv \\ = {} & \int_s \left([\boldsymbol{E} \times [(\nabla\phi) \times \boldsymbol{a}]] + \boldsymbol{E}(\boldsymbol{a}\nabla\phi)\right. \\ & \left. - \phi\boldsymbol{a} \times (i\omega\mu/c\boldsymbol{H} - 4\pi/c\boldsymbol{J}^*)\right)\boldsymbol{n}\ da.\end{aligned} \tag{11}$$

We have identically

$$\begin{aligned}\boldsymbol{n}[\boldsymbol{E} \times [\nabla\phi\boldsymbol{a}]] = \boldsymbol{a}[\nabla\phi \times [\boldsymbol{E} \times \boldsymbol{n}]], \\ [\boldsymbol{a} \times \boldsymbol{H}]\boldsymbol{n} = \boldsymbol{a}[\boldsymbol{H} \times \boldsymbol{n}].\end{aligned} \tag{12}$$

The next relationship follows from equations (11) and (12):

$$\begin{aligned}\int_v & \left(i\omega\mu/c\phi\boldsymbol{a}(4\pi/c\boldsymbol{J} + [\nabla \times (ln\mu) \times \boldsymbol{H}])\right. \\ & \left. - 4\pi/c\nabla \times \boldsymbol{J}^*\right) + (\boldsymbol{a}\nabla\phi)\nabla\boldsymbol{E})dv \\ = {} & \int_s \left(\boldsymbol{a}[(\nabla\phi) \times [\boldsymbol{E} \times \boldsymbol{n}]] + \boldsymbol{n}\boldsymbol{E}(\boldsymbol{a}\nabla\phi)\right. \\ & \left. + i\omega\mu/c\phi\boldsymbol{a}[\boldsymbol{n} \times \boldsymbol{H}] + 4\pi/c\phi\boldsymbol{a}[\boldsymbol{J}^* \times \boldsymbol{n}]\right)da.\end{aligned} \tag{13}$$

Vector $\boldsymbol{a}$ is a common factor at the both sides of equation (13). Because vector $\boldsymbol{a}$ is arbitrary, it follows from equation (13) that

$$\begin{aligned}\int_v & \left(i\omega\mu/c(4\pi/\boldsymbol{c}\boldsymbol{J} + [\nabla(ln\mu) \times \boldsymbol{H}])\phi - 4\pi/\boldsymbol{c}\nabla \times \boldsymbol{J}^*\phi\right. \\ & \left. + (\nabla\boldsymbol{E})\nabla\phi\right)dv \\ = {} & \int_s [i\omega\mu/c[\boldsymbol{n} \times \boldsymbol{H}]\phi + [\boldsymbol{n} \times \boldsymbol{E}] \times \nabla\phi + (\boldsymbol{n}\boldsymbol{E})\nabla\phi \\ & + 4\pi/\boldsymbol{c}[\boldsymbol{J}^* \times \boldsymbol{n}]\phi]da.\end{aligned} \tag{14}$$

The identity [*Stratton*, 1941]

$$\int_v [\nabla \times \boldsymbol{J}^*]\phi dv = \int_s [\boldsymbol{n} \times \boldsymbol{J}^*]\phi da + \int_v [\boldsymbol{J}^* \times \nabla\phi] dv \tag{15}$$

reduces equation (14) to

$$\int_v (i\omega\mu(\boldsymbol{J} + [\nabla(ln\mu) \times \boldsymbol{H}])\phi - [\nabla \times \boldsymbol{J}^*]\phi + (\nabla \boldsymbol{E})\nabla\phi) dv = \int_s [i\omega\mu[\boldsymbol{n} \times \boldsymbol{H}]\phi + [\boldsymbol{n} \times \boldsymbol{E}] \times \nabla\phi + (\boldsymbol{nE})\nabla\phi] da. \tag{16}$$

The exclusion of the singularity at $r = 0$ may be fulfilled using the method that was described by *Stratton* [1941]. Under an assumption that the function ϕ has the form $\phi = e^{ik\Phi(r)}/r$ within a sphere of small radius r, which is circumscribed about the point (x', y', z'), a value of $\nabla\phi$ may be estimated

$$\nabla\phi = \boldsymbol{n_o}[1/r - ikd\Phi(r)/dr]]e^{ik\Phi(r)}/r, \tag{17}$$

where $\boldsymbol{n_o}$ is unit normal to the spherical surface directed toward the center of the sphere. The form of the function $\Phi(r)$ does not have principal importance besides the requirements $\Phi(r) \to 0$, and $d\Phi(r)/dr$ is bounded if $r \to 0$. The area of the sphere vanishes with the radius as $4\pi r^2$, and since

$$[\boldsymbol{n_o} \times \boldsymbol{E}] \times \boldsymbol{n_o} + (\boldsymbol{n_o E})\boldsymbol{n_o} = \boldsymbol{E}, \tag{18}$$

the contribution of the spherical surface to the right-hand side of equation (9) is reduced to $4\pi \boldsymbol{E}(x', y', z')$. The value of $\boldsymbol{E}$ at any interior point of V is therefore (accounting for equation (3)):

$$\boldsymbol{E}(A) = -(4\pi)^{-1}\int_s \{i\omega\mu/c[\boldsymbol{n} \times \boldsymbol{H}]\phi + [\boldsymbol{n} \times \boldsymbol{E}] \times \nabla\phi + (\boldsymbol{nE})\nabla\phi\} da + \boldsymbol{E_v}(A),$$

$$\boldsymbol{E_v}(A) = (4\pi)^{-1}\int_v (4\pi/c(i\omega\mu/c\boldsymbol{J}\phi - \boldsymbol{J}^* \times \nabla\phi) + 4\pi\varepsilon^{-1}\rho\nabla\phi + i\omega/c[\nabla\mu \times \boldsymbol{H}]\phi - (\nabla(ln\varepsilon)E)\nabla\phi) dv. \tag{19}$$

An obvious interchange of vectors leads to the corresponding expression for $\boldsymbol{H}(A)$:

$$\boldsymbol{H}(A) = (4\pi)^{-1}\int_s \{i\omega\varepsilon/c[\boldsymbol{n} \times \boldsymbol{E}]\phi - [\boldsymbol{n} \times \boldsymbol{H}] \times \nabla\phi - (\boldsymbol{nH})\nabla\phi\} da + \boldsymbol{H_v}(A),$$

$$\boldsymbol{H_v}(A) = (4\pi)^{-1}\int_v (4\pi/c(i\omega\varepsilon/c\boldsymbol{J}^*\phi + \boldsymbol{J} \times \nabla\phi) + 4\pi\mu^{-1}\rho^*\nabla\phi - i\omega/c[\nabla\varepsilon \times \boldsymbol{E})\phi - (\nabla(ln\mu)H)\nabla\phi) dv. \tag{20}$$

Equations (19) and (20) describe the electric and magnetic fields $\boldsymbol{E}(A)$, $\boldsymbol{H}(A)$ at an observation point A in a general case for the inhomogeneous distributions of the electric permittivity ε and magnetic permeability μ. The terms in the right sides of equations (19) and (20) containing the external currents $\boldsymbol{J}^*$, $\boldsymbol{J}$, and charges ρ^*, ρ can be considered as the radio waves propagating from the source of emission.

[6] Let us assume that inhomogeneities are occupying only a part inside the volume V. The surface S and remaining part of volume V are located in the homogeneous medium. Then the surface integrals of equations (19) and (20) represent the contributions of the sources located outside S. If S recedes to infinity in the homogeneous medium, it may be assumed that these contributions vanish [*Stratton*, 1941]. Discarding the densities of magnetic charges and currents, one obtains from equations (19) and (20) the formulas

$$\boldsymbol{E}(A) = (4\pi)^{-1}\int_v (4\pi i\omega\mu/c^2\boldsymbol{J}\phi + 4\pi\varepsilon^{-1}\rho\nabla\phi + i\omega/c[\nabla\mu \times \boldsymbol{H}])\phi - (\nabla(ln\varepsilon)\nabla\phi) dv \tag{21}$$

and

$$\boldsymbol{H}(A) = (4\pi)^{-1}\int_v (4\pi/c\boldsymbol{J} \times \nabla\phi + i\omega/c[\boldsymbol{E} \times \nabla\varepsilon]\phi - (\nabla(ln\mu)\boldsymbol{H})\nabla\phi) dv. \tag{22}$$

Vector equations (21) and (22) depend on the Green function for inhomogeneous medium ϕ and are different from that developed by *Müller* [1969] and *Ström* [1991]. Equations elaborated by *Müller* [1969] and *Ström* [1991] include the volume integration on the inhomogeneous part of the medium but contain the Green function for free space. For the case of homogeneous medium, $\nabla(\ln\mu) = \nabla(\ln\varepsilon) = 0$ and the volume integrals (21) and (22) can be transformed into the known formulas published by *Stratton* [1941]:

$$\boldsymbol{E}(A) = \int_v (i\omega\mu/c^2\boldsymbol{J}\exp(ikr)/r + \rho/\varepsilon\nabla\exp(ikr)/r) dv \tag{23}$$

$$\boldsymbol{H}(A) = \int_v (1/c\boldsymbol{J} \times \nabla\exp(ikr)/r) dv. \tag{24}$$

The difference between propagation in the inhomogeneous medium and free space is clearly seen from equations (21), (22), (23), and (24). To find the field in the inhomogeneous medium, one might determine the Green function ϕ of the scalar wave equation (6) and then evaluate the volume integrals (21) and (22). The second terms in the volume integrals (21) and (22)

depend on the polarization of the radio waves and the direction of the refractivity gradient. If the electric field is perpendicular to the gradient of the refractivity, then the contribution of the respective part of the volume integral (21) vanishes. It follows that the secondary parts of the volume integrals (21) and (22) mainly describe the changes of the directions of the electric and magnetic vectors in the transverse radio waves, owing to the refraction effect in the layered atmosphere. The volume integrals (21) and (22) can also account for different polarization effects, e.g., the Faraday effect in the ionosphere, scattering on the atmospheric or ionospheric turbulence, etc.

[7] Now we will consider the case when the surface S is located between the transmitter and receiver. In this case the volume V contains no external sources of charges and currents within its interior or at its boundary S, then the fields at an interior point A are (if μ = const)

$$\begin{aligned} \boldsymbol{E}(A) &= -(4\pi)^{-1}\int_s \{i\omega\mu/c[\boldsymbol{n}\times\boldsymbol{H}]\phi + [\boldsymbol{n}\times\boldsymbol{E}] \\ &\quad \times \boldsymbol{\nabla}\phi + (\boldsymbol{nE})\boldsymbol{\nabla}\phi\}da + \boldsymbol{E_v}(A); \\ \boldsymbol{E_v}(A) &= -(4\pi)^{-1}\int_v (\boldsymbol{\nabla}(ln\varepsilon)\boldsymbol{E})\boldsymbol{\nabla}\phi dv, \end{aligned} \tag{25}$$

$$\begin{aligned} \boldsymbol{H}(A) &= (4\pi)^{-1}\int_s \{i\omega\varepsilon/c[\boldsymbol{n}\times\boldsymbol{E}]\phi - [\boldsymbol{n}\times\boldsymbol{H}] \\ &\quad \times \boldsymbol{\nabla}\phi - (\boldsymbol{nH})\boldsymbol{\nabla}\phi\}da + \boldsymbol{H_v}(A); \\ \boldsymbol{H_v}(A) &= -(4\pi)^{-1}\int_v i\omega/c[\boldsymbol{\nabla}\varepsilon\times E]\phi dv. \end{aligned} \tag{26}$$

[8] The last terms in the right sides of equations (25) and (26) describe the contribution of the inhomogeneous volume. If the surface S and volume V are located in the homogeneous part of the space, then one obtains the vector equations developed early by Stratton and Chu [*Stratton*, 1941]:

$$\begin{aligned} \boldsymbol{E}(A) &= -(4\pi)^{-1}\int_s \{i\omega\mu/c[\boldsymbol{n}\times\boldsymbol{H}]\phi + [\boldsymbol{n}\times\boldsymbol{E}]\times\boldsymbol{\nabla}\phi \\ &\quad + (n\boldsymbol{E})\boldsymbol{\nabla}\phi\}da, \end{aligned} \tag{27}$$

$$\begin{aligned} \boldsymbol{H}(A) &= (4\pi)^{-1}\int_s \{i\omega\varepsilon/c[\boldsymbol{n}\times\boldsymbol{E}]\phi - [\boldsymbol{n}\times\boldsymbol{H}]\times\boldsymbol{\nabla}\phi \\ &\quad - (\boldsymbol{nH})\boldsymbol{\nabla}\phi\}da,\ \phi = e^{+ikr}/r. \end{aligned} \tag{28}$$

The Stratton-Chu formulas (27) and (28) give the solution of the direct problem: to define the fields inside the homogeneous volume V if the fields propagating from the sources of radio emission are known on the interface S. Equations (25) and (26) give the solution of the direct problem for the case of inhomogeneous media. Thus the relationships (25) and (26) generalize the Stratton-Chu vector equations for description of radio waves propagation in an arbitrary inhomogeneous volume. To evaluate the vectors of electromagnetic field from equations (25) and (26), it is necessary to find the Green function of 3-D scalar wave equation (6) for an inhomogeneous medium. This task is simpler than solution of the vector Maxwell equations (2) and (3) for electromagnetic fields. This solution can be found by different ways, depending on the expected structure of the medium (e.g., WKB method for layered medium, parabolic equation methods, and geometrical diffraction methods [*Kravtsov and Orlov*, 1990; *Lukin and Palkin*, 1982]).

[9] The relationships (25) and (26) can be applied to solution of different radio science problems: scattering of the radio waves on rough surfaces with accounting for the atmospheric influence [*Pavelyev and Kucherjavenkov*, 1978], bistatic polarimetric radiolocation of Earth surface from space [*Pavelyev et al.*, 1996], subsurface radiolocation, etc. For GPS occultation the accuracy of the scalar theory corresponds to the accuracy of the measurements, and the scalar theory is quite satisfactory for the case of quiet ionosphere. The most significant factor that affects the polarization is the reflection from the surface. The use of vector theory can thus be important for the investigation of Earth's atmosphere by detecting the surface reflections [*Pavelyev and Yeliseyev*, 1989]. The possible application also consists of modeling of radio waves propagation through the ionosphere and atmosphere in different frequency bands with accounting for polarization changes connected with Faraday effect in the ionosphere and scattering on the hydrometeors in the atmosphere. Equations (25) and (26) are important for exact evaluation of the influence of 3-D structures in the electron density in the disturbed ionosphere on the polarization, amplitude, and phase of the RO signal.

3. Vector Equations for Radio Fields in the 3-D Inhomogeneous Medium (Back Propagation)

[10] For simplicity, let us chose the surface S, which contains two parallel planes S_1, S_2 from opposite sides of the atmosphere and ionosphere (Figure 2). These planes are perpendicular to plane POG (Figure 2). GPS transmitter is located in the plane POG (Figure 2) outside the volume V between the planes S_1, S_2. It is important to consider two cases: (1) homogeneous and

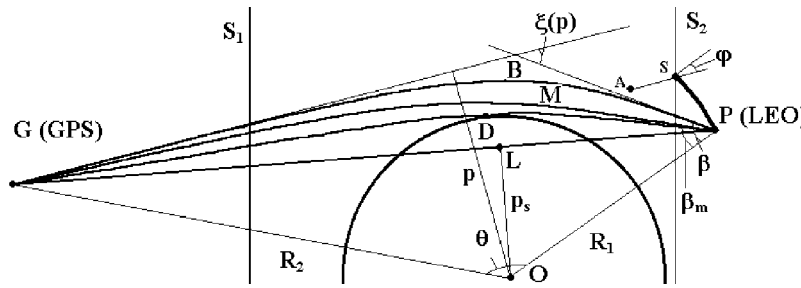

Figure 2. Scheme of the radio holographic remote sensing.

(2) inhomogeneous medium. In case (1) the wave equation (6) has two solutions $\phi^+ = e^{+ikr}/r$ (for direct-propagating waves) and $\phi^- = e^{-ikr}/r$ (for back-propagating radio waves) [*Vladimirov*, 1971]. If the Green function ϕ^+ is chosen in equations (27) and (28), then the contribution of the surface S_2 to the fields $\boldsymbol{E}(A)$, $\boldsymbol{H}(A)$ is equal to zero [*Stratton*, 1941]. Only the surface S_1 gives contribution to the fields $\boldsymbol{E}(A)$, $\boldsymbol{H}(A)$ inside the volume V. Thus the waves, propagating in the forward direction, depend on the field distribution on the surface S_1 and do not depend on the field distribution on the surface S_2. This is clear from a physical point of view because in the homogeneous medium, any gradients of the physical parameters, scattering, and reflections in the back direction are absent at the surface S_2. *Stratton* [1941] did not consider the case of back propagation corresponding to the Green function ϕ^-. However, this case may be considered by a similar way. For the Green function ϕ^-, which corresponds to the back-propagating radio waves, only the surface S_2 gives the contribution to the fields $\boldsymbol{E}(A)$, $\boldsymbol{H}(A)$ inside the volume V. Thus two different types of equations exist for the direct and back-propagating radio waves in the case of a homogeneous medium.

$$\boldsymbol{E_d}(A) = -(4\pi)^{-1}\int_{s1}\{i\omega\mu[\boldsymbol{n}\times\boldsymbol{H}]\phi^+ + [\boldsymbol{n}\times\boldsymbol{E}]\times\nabla\phi^+ + (\boldsymbol{nE})\nabla\phi^+\}da, \tag{29}$$

$$\boldsymbol{H_d}(A) = (4\pi)^{-1}\int_{s1}\{i\omega\varepsilon[\boldsymbol{n}\times\boldsymbol{E}]\phi^+ - [\boldsymbol{n}\times\boldsymbol{H}]\times\nabla\phi^+ - (\boldsymbol{nH})\nabla\phi^+\}da, \tag{30}$$

$$\phi^+ = e^{+ikr}/r, \tag{31}$$

$$\boldsymbol{E_b}(A) = -(4\pi)^{-1}\int_{s2}\{i\omega\mu[\boldsymbol{n}\times\boldsymbol{H}]\phi^- + [\boldsymbol{n}\times\boldsymbol{E}]\times\nabla\phi^- + (\boldsymbol{nE})\nabla\phi^-\}da, \tag{32}$$

$$\boldsymbol{H_b}(A) = (4\pi)^{-1}\int_{s2}\{i\omega\varepsilon[\boldsymbol{n}\times\boldsymbol{E}]\phi^- - [\boldsymbol{n}\times\boldsymbol{H}]\times\nabla\phi^- - (\boldsymbol{nH})\nabla\phi^-\}da, \tag{33}$$

$$\phi^- = e^{-ikr}/r. \tag{34}$$

Equations (29), (30), (32), (33), and Green functions (31) and (34) describe the electric and magnetic fields $\boldsymbol{E_d}(A)$, $\boldsymbol{H_d}(A)$; $\boldsymbol{E_b}(A)$, $\boldsymbol{H_b}(A)$ for the direct- and back-propagation cases if the distribution of the electromagnetic fields is known at the surface S_1 or S_2, respectively. The surface integrals (32) and (33), including the Green function ϕ^-(34), may be named as 3-D vector diffractive integrals describing the back-propagation of radio waves in a homogeneous medium.

[11] It is convenient to consider the case (2) under an assumption that both surfaces S_1 and S_2 are located within the homogeneous medium and the inhomogeneous part of space is disposed inside the volume V. Under this assumption the consideration of the case (2) is similar to one provided for the case (1). As a result, one can obtain for the direct- and back-propagation fields in an inhomogeneous medium

$$\boldsymbol{E}_d(A) = -(4\pi)^{-1}\int_{s1}\{i\omega\mu/c[\boldsymbol{n}\times\boldsymbol{H}]\phi^+ + [\boldsymbol{n}\times\boldsymbol{E}]\times\nabla\phi^+ + (\boldsymbol{nE})\nabla\phi^+\}da + \boldsymbol{E_{vd}}(A);$$
$$\boldsymbol{E_{vd}}(A) = -(4\pi)^{-1}\int_v(\nabla(ln\varepsilon)\boldsymbol{E})\nabla\phi^+dv, \tag{35}$$

$$\boldsymbol{H}_d(A) = (4\pi)^{-1}\int_{s1}\{i\omega\varepsilon/c[\boldsymbol{n}\times\boldsymbol{E}]\phi^+ - [\boldsymbol{n}\times\boldsymbol{H}]\times\nabla\phi^+ - (\boldsymbol{nH})\nabla\phi^+\}da + \boldsymbol{H}_{vd}(A),$$
$$\boldsymbol{H_{vd}}(A) = -(4\pi)^{-1}\int_v i\omega/c[\nabla\varepsilon\times\boldsymbol{E}]\phi^+dv. \tag{36}$$

$$\boldsymbol{E}_b(A) = -(4\pi)^{-1}\int_{s2}\{i\omega\mu/c[\boldsymbol{n}\times\boldsymbol{H}]\phi^- + [\boldsymbol{n}\times\boldsymbol{E}] \times \boldsymbol{\nabla}\phi^- + (\boldsymbol{nE})\boldsymbol{\nabla}\phi^-\}da + \boldsymbol{E}_{vb}(A);$$

$$\boldsymbol{E}_{vb}(A) = -(4\pi)^{-1}\int_v (\boldsymbol{\nabla}(ln\varepsilon)\boldsymbol{E})\boldsymbol{\nabla}\phi^- dv, \qquad (37)$$

$$\boldsymbol{H}_b(A) = (4\pi)^{-1}\int_{s2}\{i\omega\varepsilon/c[\boldsymbol{n}\times\boldsymbol{E}]\phi^- - [\boldsymbol{n}\times\boldsymbol{H}] \times \boldsymbol{\nabla}\phi^- - (\boldsymbol{n}\times\boldsymbol{H})\times\boldsymbol{\nabla}\phi^- - (\boldsymbol{nH})\nabla\phi^-\}da + \boldsymbol{H}_{vb}(A),$$

$$\boldsymbol{H}_{vb}(A) = -(4\pi)^{-1}\int_v i\omega/c[\boldsymbol{\nabla}\varepsilon\times\boldsymbol{E}]\phi^- dv. \qquad (38)$$

Equations (35) and (36) describe the field of the direct-propagating radio waves (index d), and equations (37) and (38) relate to the case of back-propagating radio waves (index b). The volume integrals (35) and (36) introduce the appending contribution to the field of the direct-propagating waves. In the case of radio occultation experiments using the GPS radio signals, the volume contribution introduces mainly the changes in the orientation of the electric and magnetic vectors because of the refraction of the transverse electromagnetic waves in the layered medium. For example, the volume integral (35) is equal to zero if the electric vector $\boldsymbol{E}$ is oriented normally to the gradient of the electric permittivity ε.

[12] The Green function ϕ^- in equations (37) and (38) must be found as a solution of the wave equation (6). In general, this solution is accounting for refraction, multi-beam propagation, diffraction, and scattering effects, and it may have a very complex form. The Green function ϕ^- can be found by approximate methods (e.g., WKB method) for regular layered structures in the atmosphere and ionosphere. Thus equations (37) and (38) present 3-D radio holographic equations to restore radio fields inside volume V using known radio fields at its boundary.

[13] Below, the correspondence between the backward equations developed by *Vladimirov* [1971], *Gorbunov et al.* [1996], and radio holographic equations (37) and (38) will be established. In the case of the 2-D homogeneous medium the Green functions $\phi^{\pm}$ of the wave equation (6) have the form [*Vladimirov*, 1971]

$$\phi^+ = i\pi H_o^{(1)}(kr); \quad \phi^- = -i\pi H_o^{(2)}(kr), \qquad (39)$$

where $H_o^{(1)}(kr)$, $H_o^{(2)}(kr)$ are the Hankel's function of the first and second kinds, having the asymptotic representations

$$H_o^{(1)}(kr) = (2/\pi kr)^{1/2}\exp(ikr - i\pi/4);$$
$$H_o^{(2)}(kr) = (2/\pi kr)^{1/2}\exp(-ikr + i\pi/4). \qquad (40)$$

For transition to the 2-D case, it is necessary to change the surface S_2 to the cylindrical surface, which intersects the plane POG along the orbital trajectory SP (Figure 2). Then it is necessary to account for the independence of the electric and magnetic fields $\boldsymbol{H}$, $\boldsymbol{E}$ in equations (37) and (38) (and the sources of the fields: electric currents and charges in the Maxwell equations (2) and (3)) on the coordinate y and to integrate it. After substituting equation (40) into equations (37) and (38), one obtains neglecting the terms $\sim(kr)^{-1/2}$

$$\boldsymbol{E_b}(A) = 0.5[k_o/(2\pi)]^{1/2}\int_{SP}\{-\mu[\boldsymbol{n}\times\boldsymbol{H}] + [\boldsymbol{n}\times\boldsymbol{E}]\times\boldsymbol{\tau} + (\boldsymbol{nE})\boldsymbol{\tau}\}\exp(i\pi/4 - ikr)/r^{1/2}dl, \qquad (41)$$

$$\boldsymbol{H_b}(A) = 0.5[k_o/(2\pi)]^{1/2}\int_{SP}\{\varepsilon[\boldsymbol{n}\times\boldsymbol{E}] + [\boldsymbol{n}\times\boldsymbol{H}]\times\boldsymbol{\tau} + (\boldsymbol{nH})\boldsymbol{\tau}\}\exp(i\pi/4 - ikr)/r^{1/2}dl, \qquad (42)$$

$$r = |\mathbf{r} - \mathbf{r}'| = \left[(x-x')^2 + (z-z')^2\right]^{1/2}, \qquad (43)$$

where k_o is the wave number corresponding to propagation of radio waves in a vacuum, and $\boldsymbol{\tau}$ is the unit vector parallel to the direction on the current integration element from the observation point.

[14] According to *Gorbunov et al.* [1996], the back-propagated field $u(x, y, z)$ is calculated using the diffractive integral:

$$u(x,y,z) = (k/2\pi)^{1/2}\int ds|\boldsymbol{r}-\boldsymbol{y}|^{-1/2}\cos\varphi\exp(i\pi/4 - ik|\boldsymbol{r}-\boldsymbol{y}|)u_o(\boldsymbol{y}), \qquad (44)$$

where $\boldsymbol{r}$, $\boldsymbol{y}$ correspond to coordinates of the observation point A and the current point of integration on the curve SP along the LEO orbit; φ is the angle between vector $\boldsymbol{r}-\boldsymbol{y}$ and normal to the curve SP (Figure 2) at the current integration point $\boldsymbol{y}$; and $u_o(\boldsymbol{y})$ is a scalar field measured along the orbit of LEO satellite. Equation (44) has been derived under the assumption that the source of the wave field (GPS) is stationary and that the LEO orbit is located in an occultation plane [*Gorbunov and Kornblueh*, 2001]. The phase factor $\exp(i\pi/4 - ikr)/r^{1/2}$ in equations (41) and (42) coincides with the phase factor in equation (44). Distinction between equations (41) and (42) and equation (44) consists of the polarization terms in the right sides of equations (41) and (42), which are depending on the directions of the electromagnetic fields measured along the curve SP (Figure 2). Thus the known 2-D scalar equation applied for the solution of the inverse radio occultation problem is a partial case of the diffractive vector integrals for 3-D inhomogeneous

medium. The 3-D equations (41) and (42) are valid for a general case when the refracted rays have deflections from the radio occultation plane because of the influence of the horizontal gradients of the refractivity in the ionosphere and atmosphere.

4. The Green Function and Reference Signal for RFSA Method

[15] Now we can establish a connection between the Green function of the 3-D wave equation and the reference signal for the RFSA method used early [*Hocke et al.*, 1999; *Igarashi et al.*, 2000, 2001; *Pavelyev et al.*, 2002a]. For achieving this aim, we will use the equations (21) and (22) under the assumption that the volume integrals terms containing gradient $\nabla(\ln\varepsilon)$, $\nabla\varepsilon$ can be neglected. This assumption is valid, e.g., if the direction of the electric field in the emitted wave is perpendicular to the radio occultation plane. The field along the LEO orbit can be presented in the form

$$\boldsymbol{E}(A) = \int_{\boldsymbol{v}} \left(i\omega\mu/c^2 \boldsymbol{J}\phi + \rho/\varepsilon \boldsymbol{\nabla}\phi\right) dv, \tag{45}$$

$$\boldsymbol{H}(A) = c^{-1} \int_{\boldsymbol{v}} \boldsymbol{J} \times \boldsymbol{\nabla}\phi dv, \tag{46}$$

where ϕ is a solution of the wave equation (6) for inhomogeneous medium corresponding to the direct wave. We assume that the field is emitted by a point source with unit intensity located at point G (Figure 2).

[16] In general, the solution of the diffraction problem in layered medium can be presented in frame of the geometrical diffraction theory [*Kravtsov and Orlov*, 1990; *Lukin and Palkin*, 1982] as a sum of the fields corresponding to M different physical rays

$$E(\boldsymbol{A}) = \boldsymbol{A_o}\phi(\boldsymbol{r}, t); \phi(\boldsymbol{r}, t) = \sum_{j=1}^{M}$$
$$A_j(p_j) \exp\left[i\left(\omega_o t - k\Phi(p_j, \boldsymbol{r}, R_2)\right)\right]; \Phi(p_j) = \int n_j(l) dl, \tag{47}$$

where $k = 2\pi/\lambda$ $\omega_o = 2\pi f_o$, f_o is the carrier frequency of radio field, $n_j(l)$ is the refraction index distribution along the jth ray trajectory, M is a number of the ray trajectories connecting points P and G (M may be a function of time depending on physical conditions in the atmosphere), $\Phi(p_j)$ is the eikonal [*Kravtsov and Orlov*, 1990], p_j is the impact parameter of the jth physical ray initiated at the source, $\boldsymbol{A_o}$ is the complex vector amplitude of the electric field depending on the intensity and phase of the source, and $A_j(p_j)$ is the complex amplitude of the jth physical ray normalized to the amplitudes corresponding to the free space propagation. $A_j(p_j)$ depends on the refraction attenuation in power of jth ray $X_j(p_j)$, $A_j(p_j) = [X_j(p_j)]^{1/2}$. In the case of spherical symmetry the refraction angle of jth physical ray can be described by equations [e.g., *Pavelyev and Yeliseyev*, 1989] (index j in these equations is omitted for simplicity of writing):

$$\xi(p) = A(p) - A(p_s),$$
$$A(p) = \sin^{-1}(p/n(R_1)R_1) + \sin^{-1}(p/n(R_2)R_2), \tag{48}$$
$$A(p_s) = \sin^{-1}(p_s/R_1) + \sin^{-1}(p_s/R_2),$$

where $\xi(p)$ is the refraction angle, p is the impact parameter of physical ray, p_s is the free space impact parameter corresponding to the free space ray GLP (Figure 2), and $n(R_2)$, $n(R_1)$ are the refraction indexes at the point G and P, respectively. The phase path excess $\Phi(p)$ (the difference between the eikonals relating to the jth ray and free space ray) may be described by expression [*Pavelyev and Yeliseyev*, 1989]

$$\Phi(p) = L_2(p) + L_1(p) - L_2(p_s) - L_1(p_s) + p\xi(p) + \kappa(p),$$
$$L_1(p) = \left(n^2(R_1)R_1^2 - p^2\right)^{1/2}, L_2(p) = \left(n^2(R_2)R_2^2 - p^2\right)^{1/2},$$
$$L_1(p_s) = \left(R_1^2 - p_s^2\right)^{1/2}, L_2(p_s) = \left(R_2^2 - p_s^2\right)^{1/2}, \tag{49}$$

where $\Phi(p)$ depends on the geometrical terms $L_1(p)$, $L_2(p)$, $L_1(p_s)$, $L_2(p_s)$, $p\xi(p)$, and main refractivity part $\kappa(p)$. The value $\kappa(p)$ is connected with refraction angle $\xi(p)$ by the relationship [*Pavelyev and Yeliseyev*, 1989]

$$d\kappa(p)/dp = -\xi(p). \tag{50}$$

The central angle θ is connected with refraction angle by equation

$$\theta(p) = \pi + \xi(p) - A(p), \tag{51}$$

where $A(p)$ is defined in equation (48). Equations (48)–(51) connect the phase and angular characteristics of the jth ray. The amplitude of the jth ray is dependent on the refraction attenuation and may be defined as a ratio $X(p)$ of the wave intensity in the medium to the intensity in the free space. *Pavelyev and Kucherjavenkov* [1978] defined the refraction attenuation as a ratio $X_e(p)$ of power flow of radio waves in the medium to the power flow in the free space. From their formula for $X_e(p)$, one can obtain the formula for $X(p)$

$$X(p) = pR_0^2[R_1R_2L_2(p)L_1(p)\sin\theta]^{-1}|\partial\theta/\partial p|^{-1}, \tag{52}$$

$$\partial\theta/\partial p = d\xi/dp - 1/L_2(p) - 1/L_1(p), \tag{53}$$

where R_0 is the distance in free space from the transmitter to the current point on the jth ray. Note that equations (48)–(53) are valid for each physical ray in multipath conditions. Equation (52) is also valid for the refraction attenuation of the reflected signal [*Pavelyev et al.*, 1997]. In general, the Green function ϕ in equation (47) can correspond to the physical rays of different origin (main ray GMP, refracted multipath rays, reflected ray GDP (Figure 2), diffracted rays, scattered rays, and others relating to various physical mechanisms) having the complex amplitude $A_j(p_j)$ and propagating at different angles β_j relative to the line PO.

[17] For the circular orbit and spherical symmetric medium, the eikonals $\Phi(p_j)$ corresponding to the refraction and reflection mechanisms have a common property [*Pavelyev et al.*, 1997]:

$$\partial\Phi(p_j)/\partial p_j = p_j \partial\theta/\partial p_j, \tag{54}$$

if R_1 = const, R_2 = const.

[18] The record of the complex radio signal $\phi(\boldsymbol{r}, t)$ along the LEO trajectory can be considered as the radio hologram's envelope that contains the amplitude $A(t)$ and phase path excess $\psi(t) = kS_e(t)$ of the radio field as the functions of time [*Pavelyev*, 1998; *Hocke et al.*, 1999; *Igarashi et al.*, 2000]:

$$\phi(r,t) = A(t)\exp[-i\psi(t)]. \tag{55}$$

The reference signal $E_m(t) = A_m^{-1}(t)\exp[i\psi_m(t)]$ must be developed to acquire maximum coherence with the RO signal. The functions $A_m(t)$ and $\psi_m(t)$ determine the parameters of the focused synthetic aperture and spatial resolution. The phase $\psi_m(t)$ and amplitude $A_m(t)$ of the reference signal must be related to the phase $\psi_c(t)$ and amplitude $A_c(t)$ of the main (coherent) part of the RO signal corresponding to the main ray GP. To achieve this, a model of refractivity in the atmosphere and ionosphere can be applied. Naturally, the model must be representative to the actual physical conditions in the radio occultation region. Without such a model the spatial resolution will correspond to an unfocused synthetic aperture (Doppler selection) and will be roughly 0.5–1 km. *Igarashi et al.* [2000, 2001] used the amplitude $A_m(t)$ = const and an exponential model to describe the refractivity profile of the atmosphere with the IRI-95 model for the ionosphere in the RO region to determine the temporal dependence of $\psi_m(t)$ and obtained a spatial resolution of about 70 m. They applied the Fourier transform to the product of the RO and reference signals to obtain the compressed angular spectrum $W(p(\omega))$ of the RO signal:

$$W(p(\omega)) = \int_{-T/2}^{T/2} dt\,\phi(\boldsymbol{r},t)A_m^{-1}(t)\exp[i\psi_m(t)]\exp(-i\omega t), \tag{56}$$

where T is the time of focused synthesis. Equation (56) describes the compressed angular spectrum of the radio field $W(p(\omega))$ as function of the ray coordinates β and p (Figure 2).

[19] Integration on time in equation (56) is equivalent to integration on the central angle θ. In the case of circular orbits of GPS and LEO satellites,

$$dt = d\theta\Omega^{-1}(p_s),$$

$$\Omega^{-1}(p_s) = \left[1/\left(R_1^2 - p_s^2\right)^{1/2} + 1/\left(R_2^2 - p_s^2\right)^{1/2}\right]/v_\perp,$$

$$v_\perp = -dp_s/dt,\ t = (\theta - \theta_o)\Omega^{-1}(p_s), \tag{57}$$

where $\Omega(p_s)$ is the angular speed of relative orbital motion of the GPS and LEO satellites, $v_\perp$ is the vertical speed of the point L, and θ_o is the central angle corresponding to the time instant $t = 0$. The eikonal can be presented as a two-term expansion at $\theta = \theta_o$, $p_o = p(\theta_o)$ if $\partial\theta/\partial p(\theta_o) \neq 0$:

$$\Phi(p(\theta)) - \Phi(p_o) = p_o(\theta - \theta_o) + 0.5(\theta - \theta_o)^2/\partial\theta/\partial p(\theta_o), \tag{58}$$

where dependence $\theta(p)$ is given by relationship (51). The condition $\partial\theta/\partial p(\theta_o) = 0$ is fulfilled at the caustics boundaries where the numbers of rays are changed by even numbers [*Lukin and Palkin*, 1982; *Kravtsov and Orlov*, 1990]. The partial derivative $\partial\theta/\partial p(\theta_o)$ in equation (58) is evaluated under conditions R_1 = const, R_2 = const.

[20] The main principle of the focused synthetic aperture approach consists of choosing the reference signal matching in the optimal sense with received signal [e.g., *Wehner*, 1987, section 6.4], so the phase of the reference signal must have the form similar to that of the phase of RO signal, corresponding to the main ray trajectory GBP (Figure 2):

$$\psi(p_m(\theta)) - \psi(p_m(\theta_o)) = p_m(\theta_o)(\theta - \theta_o) + 0.5(\theta - \theta_o)^2 / (\partial\theta/\partial p(\theta_o))_m, \tag{59}$$

where $p_m(\theta_o)$, $p(\theta)$, and $(\partial\theta/\partial p(\theta_o))_m$, $\partial\theta/\partial p(\theta_o)$ are the impact parameters and the partial derivatives, respectively, corresponding to the reference signal and physical ray at the time instant $t = 0$. After substituting equations (58) and (59) in equation (56), we can obtain:

$$W(\omega) = \int_{-T/2}^{T/2} dt\phi(\boldsymbol{r},t)A_m^{-1}(t)\exp[i\psi_m(t)]\exp(-i\omega t) = \sum_{j=1}^{M_1} f(\omega, p_j), \tag{60}$$

$$f(\omega,p_j)=\int_{-\Delta/2}^{\Delta/2} d\theta\Omega^{-1}(p_s)\left[X_j(p_j)/X_m(p_m)\right]^{1/2}\cdot\exp\left\{i\left[q(\theta-\theta_o)-k\left(\Phi(p_{jo})+\psi_m(p_{mo})\right)+ks(\theta-\theta_o)^2\right]\right\},\quad(61)$$

$$q=(\omega_o-\omega)\Omega^{-1}(p_s)+k(p_m-p_j);$$
$$s=0.5\left[1/(\partial\theta/\partial p)_m-1/(\partial\theta/\partial p)_j\right],\quad(62)$$
$$\Delta=T\Omega(p_s),$$

where $f(\omega, p_j)$ describes the response of the focused synthetic aperture to the jth physical ray, and Δ is the interval of integration on θ. Usually the reference signal is chosen to maximize the response $f(\omega, p_j)$ for coherent part of the RO signal, corresponding to the main ray GBP (Figure 2) and having the impact parameter p. To accomplish this end, the refraction attenuation and the phase of the reference signal must be close to the same parameters of the coherent part of RO signal:

$$X_m(p_m)\approx X(p),(\partial\theta/\partial p)_m\approx\partial\theta/\partial p.\quad(63)$$

Two conditions (equation (63)) can be fulfilled simultaneously because the refraction attenuation significantly depends on the partial derivative $\partial\theta/\partial p$ (equation (53)). It follows from condition (63) and equations (56) and (58)–(60) that the variations in the phase of the reference signal must be equal to the variations in the phase of the Green function, and the amplitude of the reference signal must change inversely with the amplitude of the Green function. This means that the focus of the focused synthetic aperture must follow the current position of the center of curvature of the wave front of the main ray (disposed at the point G (Figure 2)) if the refractivity model is exact. If the amplitude and phase of reference signal are chosen according to condition (63), then the function $f(\omega, p)$ has a form:

$$f(\omega,p)=i\Delta[\sin(q\Delta/2)]/(q\Delta/2),$$
$$q=(\omega_o-\omega)\Omega^{-1}(p_s)+k(p_m(\theta_o)-p(\theta_o)).\quad(64)$$

This function has sharp maximum at the frequency $\omega-\omega_o$ equal to

$$\omega-\omega_o=k\Omega(p_s)(p(\theta_o)-p_m(\theta_o)).\quad(65)$$

Then we can estimate the impact parameter $p(\theta_o)$ using given values $p_m(\theta_o)$ and $\Omega(p_s)$

$$p(\theta_o)=(\omega-\omega_o)/[k\Omega(p_s)]+p_m(\theta_o).\quad(66)$$

Thus the found impact parameter $p(\theta_o)$ is a sum of the impact parameter $p_m(\theta_o)$ corresponding to the model of the refractivity used for the construction of the reference signal and small part corresponding to deflection of the maximum value of Fourier component of convolution of the reference and RO signals.

[21] The accuracy of the estimation $\delta p(\theta_o)$ depends on the width of the maximum δ_o, which is determined by the parameters $\Omega(p_s)$ and Δ. One obtains $\delta p(\theta_o)$ using the relationship (62) for q and Δ and equations (64)–(66):

$$\delta_o=\pi\Omega(p_s)/\Delta;$$
$$\delta_p(\theta_o)=\delta_o/[k\Delta\Omega(p_s)]=\lambda/\{Tv_\perp[1/L_1(p_s)+1/L_2(p_s)]\}=\lambda R_1/L_a,\quad(67)$$
$$L_a=Tv,\quad(68)$$

where L_a is the size of the focused synthetic aperture, and v in equation (68) is practically equal to the orbital speed of the LEO satellite. Equations (67) and (68) give relationships describing the extreme value for the vertical resolution in the impact parameter $p(\theta_o)$ corresponding to the case when the amplitude and phase of reference signal are in full accordance with the phase and amplitude of the RO signal. For numerical estimation, we can let L_a = 20 km, v = 8 km/s, T = 2.5 s, λ = 20 cm, and R_1 = 7000 km, then we obtain from equation (67) that $\delta p(\theta_o)$ = 70 m. One can obtain the estimation of the refraction angle $\xi(\theta_o)$ by substituting the found value p and known impact parameter p_s into equation (48) [*Hocke et al.*, 1999].

[22] Note that the considered method can evaluate also the amplitude and phase for each ray in the Green function spectrum (47) using the relationships (60)–(62) and choosing the appropriate form for the reference signal. Thus the radio holographic focused synthetic aperture method (RFSA), developed early by *Pavelyev* [1998], *Hocke et al.* [1999], *Igarashi et al.* [2001], and *Pavelyev et al.* [2002a], is justified as a method, which uses the phase and amplitude of the Green function for the construction of the reference signal.

[23] The distinction of practical application of the RFSA method for the radar and atmospheric case mainly consists of the different spatial position of the focus of the synthesized aperture. In the radar case, this place coincides with a target on Earth surface or in the atmosphere. In the case of the atmospheric investigation the targets are the rays emitted by transmitter and a position of the focus of the synthesized aperture coincides with the current position of the curvature center of the corresponding wave front. The task in the radar case consists of the precise determination of the position of a target. The task in the atmospheric investigation is the accurate evaluation of the impact parameters of the rays

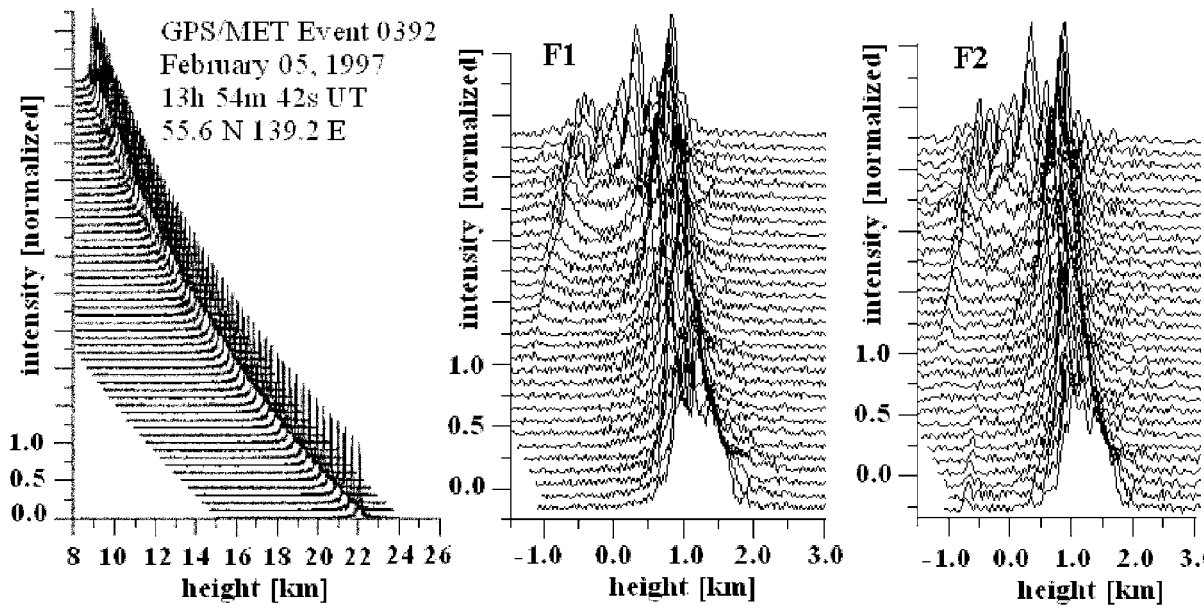

Figure 3. Radio images of the atmosphere obtained by the RFSA method. (left) Radio images of the lower stratosphere and upper troposphere. Radio images of the boundary layer of the troposphere at frequencies (middle) F1 and (right) F2. The radio images are given in sequence with time interval 0.32 s. The length of the focused synthetic aperture is ~20 km; this corresponds to the expected value of vertical resolution ~70 m at the distance ~3000 km.

and the corresponding refraction angles [*Hocke et al.*, 1999; *Igarashi et al.*, 2000; *Pavelyev et al.*, 2002a, 2002b].

[24] Equation (56) can be used for obtaining the radio images of the atmosphere and terrestrial surface because connection (65) between the frequency ω and the physical ray impact parameter p is valid owing to coherence of the rays emitted by the GPS transmitter. The increasing of the difference in the partial derivatives s (equation (62)) introduced broadening in the main maximum of the function $f(\omega, p_j)$ (equation (62)) and does not change the position of the maximum. Only near the caustic surfaces where the partial derivative $\partial\theta/\partial p$ is close to zero, the radio image can blur owing to broadening of the angular spectrum of the radio waves.

[25] Examples of radio images of the atmosphere and Earth's surface are shown in Figure 3. For construction of the reference signal, an exponential model of the refractivity has been used: $N(h) = N_o \exp(-h/H)$, N_o = 300 (N units), H = 6.3 km. This model corresponds to single-beam propagation. The images relate to RO event 0392 (5 February 1997; 1354 UT; 56°N, 139°E). The radio images of the stratosphere in the height interval 8–22 km (Figure 3) contain mainly sharp peaks having vertical width ~70 m at the half power level. It corresponds to an angular resolution of about 17–23 microradians and spatial compression of the RO signal ~1/10 of the Fresnel zone size. The radio brightness distribution in the boundary layer at a height of 0–2 km is shown in Figure 3. Negative height values correspond to the signals reflected from Earth's surface. The main peak corresponds to a radio occultation signal propagating along the path GBP (Figure 2). In the boundary layer of the troposphere shown in Figure 3, the spatial compression effect in the main peak is variable because influence of multipath propagation. The weak reflected signal is slowly moving toward the main tropospheric signal. The behavior of the reflected signal is similar at both GPS frequencies F1 and F2, thus indicating minimal level of the possible systematic receiver's errors. The width of the peaks of the reflected signals changed in the interval 100–500 m depending on the time (Figure 3). The maximal width of the tropospheric signal in the boundary layer is ~700–1000 m. The minimal width of spikes in the tropospheric signal is about of 100 m. These spikes correspond to the terminal part of the RO event when the main tropospheric signal is transformed to two sharp peaks, which are clearly seen both at frequencies F1 and F2 (Figure 3). It follows from Figure 3 that the vertical resolution of the RFSA method depends on the degree of coherence of the reference signal with main RO signal and can be about 70–100 m. The RFSA method allows one to observe the effects of the multibeam propagation, which are important for the

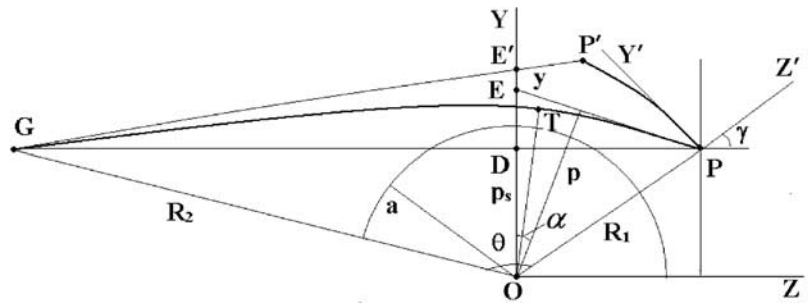

Figure 4. Geometrical parameters for the GIO, RFSA, CT, and BP methods. PP′ is the orbital trajectory of LEO satellite.

theory of radio wave propagation in the atmosphere and in its boundary layer.

5. GIO, RFSA, CT, and BP Methods

[26] To reveal connections between RFSA, CT, and BP methods, we apply the Zverev's transform [*Zverev*, 1975], connecting the field $E(y, z)$ and its angular spectrum $A(\alpha)$

$$E(y,z) = \int d\alpha A(\alpha) \exp\{ik[\Phi(\alpha,y,z) - \Phi_j(\alpha)]\},$$
$$\Phi(\alpha,y,z) = z\cos\alpha + y\sin\alpha, \Phi_j(\alpha) = \Phi(\alpha,y_j,z_j), \quad (69)$$

where $\Phi(\alpha)$, $\Phi_j(\alpha)$, y_j, z_j are the phase function, initial phase, and initial coordinates of the jth physical ray. The center of coordinate system y, z coincides with point O, and axis OY is perpendicular to direction GP (Figure 4). Integral (69) can be evaluated by method of the stationary phase (SP) as the sum of the fields of the physical rays similar to equation (47) in the free space. We introduce GIO transform $I(p)$:

$$I(p) = k/2\pi \int d\eta B(\eta) \exp ik[pf(\eta) - d(\eta)] I_1(\eta),$$
$$I_1(\eta) = \int ds \exp(-ik\eta s) R(s) E(y(s), z(s)), \quad (70)$$

where $I_1(\eta)$ is the internal operator, $R(s)$ is the reference signal, $B(\eta)$ is the amplitude function, $d(\eta)$ is the auxiliary phase function, $f(\eta)$ is the impact function, p is the parameter, having different physical interpretation depending on $f(\eta)$, and s is the path of integration along the orbital trajectory of the LEO satellite.

[27] The GIO transform can be considered as a generalization of the Egorov's Fourier integral operator [*Egorov*, 1985]. The reference signal $R(s)$ is included in GIO with aim to compress the angular spectrum and to account for the form of the orbital trajectory. The functions $f(p,\eta)$, $B(p,\eta)$, $d(\eta)$ can be arbitrary, and their physical meaning can be revealed using Zverev's presentation for the field (equation (69)). The RFSA method uses only the operator $I_1(\eta)$ with the reference signal $R(s) = E_m(t(s))$ in equation (70) and the field presentation in the form (47) as shown in section 4. The RFSA method can retrieve the field along the curved rays (e.g., rays P′E′, PE in Figure 4) with some approximation depending on the degree of spatial compression achieved. The RFSA method can reconstruct the phase and amplitude of the fields in the plane GOY (Figure 4) and thus obtain the 1-D radio images of the atmosphere and terrestrial surface. The RFSA method can account for the motion of GPS transmitter in any direction and influence of the horizontal gradients in the ionosphere and atmosphere by means of their introducing to the refractivity model. However, the RFSA method requires algorithms for solving the direct-propagation problem with accounting for the diffraction effect to achieve maximal spatial compression with aim to apply the perturbation method to find from experimental data correction to the refractivity profiles.

[28] To obtain connection between the GIO, BP, and CT methods, we introduce the new coordinate system y', z' with center at point P and oriented at angle γ relative to the coordinate system y, z (Figure 4). The coordinate y′ is reckoned from point P along the tangent to orbital trajectory of LEO satellite. The coordinates y, z and y', z' are connected by equation

$$y = y_p + y'\cos\gamma + z'\sin\gamma, \; z = z_p + z'\cos\gamma - y'\sin\gamma, \quad (71)$$

where y_p, z_p are the coordinates of the point P in the coordinate system ZOY (Figure 4). Now we can substitute the integration variable y' instead of s in the operator $I_1(\eta)$. After substituting equations (69) and (71) into equation (70) and changing the order of the integral

operators one can perform integration on y' letting $z' = 0$, $R(s) = 1$:

$$I_1(\eta) = k/2\pi \int dy' \exp\{-iky'[\eta - \sin(\alpha - \gamma)]\} = \delta(\eta - \sin(\alpha - \gamma)). \quad (72)$$

Integration on η in equation (70) gives

$$E(p) = \int d\alpha A(\alpha) \exp\{ik[\, pf(\eta(\alpha)) - d(\eta(\alpha)) + z_p \cos\alpha + y_p \sin\alpha - \Phi_j(\alpha))]\} B(\eta(\alpha)), \quad \eta(\alpha) = \sin(\alpha - \gamma). \quad (73)$$

The left part of equation (73) is the field $E(p)$ transformed by the operator $I(p)$ from the RO signal. The function $d(\eta)$ in equation (70) is arbitrary, and one can chose $d(\eta)$ in the GIO transform (70) to simplify equation (73):

$$d(\eta) = z_p \cos\left(\gamma + \sin^{-1}\eta\right) + y_p \sin\left(\gamma + \sin^{-1}\eta\right). \quad (74)$$

If the origin of the coordinate system y', z' is disposed at the OZ axis and $\gamma = 0$, $y_p = 0$, then the function $d(\eta)$ is equal to $z_p(1 - \eta^2)^{-1/2}$ and coincides with the phase of the transfer function for free space introduced early [*Zverev*, 1975].

[29] The BP case can be obtained from equation (73) by choosing the impact function $f(\eta) = \sin(\gamma + \sin^{-1}\eta)$ in the GIO transform (70). In this case, equation (73) coincides with equation (69), if $z = 0$, and, as a consequence, corresponds to the distribution of the field along the straight line OY, and p has a geometrical sense of the coordinate y (Figure 4). The second important partial case is $f(\eta) = \gamma + \sin^{-1}\eta$. For the case $\gamma = 0$, this function has been found early by the CT method [*Gorbunov*, 2002c]. For the second case the SP method gives a connection between the direction angle α_j and parameter p

$$p = -z_j \sin\alpha_j + y_j \cos\alpha_j. \quad (75)$$

Equation (74) defines p as the distance between the jth physical ray and the center of the coordinate system, point O (Figure 4). If the center of global spherical symmetry of the medium coincides with point O, then p is the impact parameter of the jth ray. The SP method gives the next formula for the transformed field

$$E(p, 0) = A(\alpha_j) C_j B(\alpha_j) \exp\left[ik\left(p\alpha_j - \Phi_j(\alpha_j)\right)\right], \quad (76)$$

where C_j is the coefficient describing contribution of the stationary point corresponding to the jth physical ray. When the modified refraction index $M(r)$ is a monotonic function, only one physical ray can correspond to the impact parameter p. A possibility of the multipath effect corresponding to monotonic $M(r)$ profiles has been shown early by *Pavelyev* [1998]. In this case the GIO can disentangle the multipath rays expressing the ray direction angle α as a single-valued function of the impact parameter p. The CT method has the same capability as a partial case of the GIO transform. The ray direction angle α can be determined from equation (76) by differentiating the phase of the field $E(p)$: $\alpha = d\arg E(p)/dp$ [*Gorbunov*, 2002c]. Note that in this case the BP method can be a subject of multipath distortion. In reality, only the centers of the local spherical symmetry exist for different parts of the ray trajectories in the ionosphere and atmosphere. In this case the phase of the field transformed by the GIO, CT, and BP methods can contain distortion connected with horizontal gradients in multipath situation [*Gorbunov*, 2002c].

6. Conclusion

[30] The main result of this paper is elaborating and preliminary analysis of the 3-D vector radio holographic equations designed to restore the field distribution in the inhomogeneous atmosphere and ionosphere. The 3-D vector equations are obtained for two practically important cases: propagation in the forward and backward directions. The equations relevant to these cases include distinct Green functions, which are solutions of the 3-D scalar wave equations for forward and backward propagated field corresponding to the point source. The new result for forward propagation consists of discovering a new form of the volume contribution depending on the Green function relevant to inhomogeneous medium, the polarization of the radio waves, and the gradient of the refractivity. This volume contribution can be important in some practical applications. In the RO investigation the volume contribution can be notable in the case of scattering on the hydrometeors or turbulence. The 3-D equations for the back-propagated field are new both for the case of homogeneous and inhomogeneous medium. In the first case they can be transformed to equation similar to the 2-D scalar equation for homogeneous medium, but a distinction exists and corresponds to vector character of the equations. It is shown that the phase of the reference signal used in the RFSA method, developed early with aim to heighten vertical resolution in analysis of the RO data, must coincide with the phase of the Green function of the scalar wave equation corresponding to 3-D inhomogeneous medium. This substantiated the RFSA principle for the atmospheric investigation using the RO data. The phase and amplitude of the reference signal are evaluated in the RFSA method using the model of the atmosphere in the RO region. This corresponds to approximate the solution of the wave equation for the Green function. Then the

necessary adjustments can be made by perturbation method. As was shown early in this paper, the RFSA method gives a possibility to find the temporal dependencies of the amplitude, phase, impact parameter, and refraction angle for each ray in the angular spectrum of the radio field. The RFSA method is free, in principle, from difficulties arising with multibeam propagation in existing methods because it can visualize the physical rays by the adaptive manner. The RFSA method can be used for obtaining radio images of the atmosphere and terrestrial surface in the RO regions with high vertical resolution $\sim$70 m. It follows from comparison of the GIO, RFSA, BP, and CT methods that the RFSA, BP, and CT methods are partial cases of the GIO transform. The GIO transform can be considered as upgraded by including the reference signal Egorov Fourier integral operator. The Zverev transform combined with the GIO transform allows one to reveal a physical sense of the CT and BP methods and to establish their limitations. In distinction with the CT method the GIO transform is valid for any inclination of the orbital trajectory of the LEO satellite in the RO plane. The GIO transform can be considered as a practical tool for the application of the Zverev and Egorov's Fourier integral operators to the analysis of the RO data. As follows from our analysis, the radio holography can be used in future after some modernization to realize highly precise GPS radio signals for the purpose of remote sensing of the atmosphere, mesosphere, and terrestrial surface with high spatial resolution and accuracy.

[31] **Acknowledgments.** We are grateful to UCAR for access to the GPS/MET data. We are grateful to National Science Council of Taiwan for financial support under the grants NSC 92-2811-M008-001, NSC 91-2111-M008-029, and Office of Naval Research (ONR) of the United States under grant N00014-00-0528. Work has been partly supported by Russian Fund of Basic Research, grant 03-02-17414.

References

Beyerle, G., and K. Hocke (2001), Observation and simulation of direct and reflected GPS signals in radio occultation experiments, *Geophys. Res. Lett.*, *28*(9), 1895–1898.

Beyerle, G., K. Hocke, J. Wickert, T. Schmidt, C. Marquardt, and C. Reigber (2002), GPS radio occultations with CHAMP: A radio holographic analysis of GPS signal propagation in the troposphere and surface reflections, *J. Geophys. Res.*, *107*(D24), 4802, doi:10.1029/2001JD001402.

Egorov, Y. V. (1985), *Lectures on Partial Differential Equations: Additional Chapters* (in Russian), Moscow State Univ. Press, Moscow.

Gorbunov, M. E. (2002a), Radio-holographic analysis of Microlab-1 radio occultation data in the lower troposphere, *J. Geophys. Res.*, *107*(D12), 4156, doi:10.1029/2001JD000889.

Gorbunov, M. E. (2002b), Radioholographic analysis of radio occultation data in multipath zones, *Radio Sci.*, *37*(1), 1014, doi:10.1029/2000RS002577.

Gorbunov, M. E. (2002c), Canonical transform method for processing radio occultation data in the lower troposphere, *Radio Sci.*, *37*(5), 1076, doi:10.1029/2000RS002592.

Gorbunov, M. E., and L. Kornblueh (2001), Analysis and validation of GPS/MET radio occultation data, *J. Geophys. Res.*, *106*(D15), 17,161–17,169.

Gorbunov, M. E., A. S. Gurvich, and L. Bengtsson (1996), Advanced algorithms of inversion of GPS/MET satellite data and their application to reconstruction of temperature and humidity, Rep. 211, Max-Planck-Inst. for Meteorol., Hamburg.

Gorbunov, M. E., A. S. Gurvich, and L. Kornblueh (2000), Comparative analysis of radio holographic methods of processing radio occultation data, *Radio Sci.*, *35*(4), 1025–1034.

Hocke, K., A. Pavelyev, O. Yakovlev, L. Barthes, and N. Jakowski (1999), Radio occultation data analysis by radio holographic method, *J. Atmos. Sol. Terr. Phys.*, *61*, 1169–1177.

Igarashi, K., A. Pavelyev, K. Hocke, D. Pavelyev, I. A. Kucherjavenkov, S. Matugov, A. Zakharov, and O. Yakovlev (2000), Radio holographic principle for observing natural processes in the atmosphere and retrieving meteorological parameters from radio occultation data, *Earth Planets Space*, *52*, 875–968.

Igarashi, K., A. Pavelyev, K. Hocke, D. Pavelyev, and J. Wickert (2001), Observation of wave structures in the upper atmosphere by means of radio holographic analysis of the radio occultation data, *Adv. Space Res.*, *27*(6–7), 1321–1327.

Jensen, A. S., M. S. Lohmann, H.-H. Benzon, and A. S. Nielsen (2003), Full spectrum inversion of radio occultation signals, *Radio Sci.*, *38*(3), 1040, doi:10.1029/2002RS002763.

Kravtsov, Y., and Y. N. Orlov (1990), *Geometrical Optics of Inhomogeneous Media*, Springer-Verlag, New York.

Kunitsyn, V. E., and E. D. Tereshchenko (1991), *Tomography of the Ionosphere* (in Russian), Nauka, Moscow.

Kunitsyn, V. E., E. S. Andreeva, E. D. Tereshchenko, B. Z. Khudukon, and T. Nygren (1994), Investigations of the ionosphere by satellite radiotomography, *Int. J. Imag. Sys. Technol.*, *5*, 112–127.

Lindal, G. F., J. R. Lyons, D. N. Sweetnam, V. R. Eshleman, D. P. Hinson, and G. L. Tyler (1987), The atmosphere of Uranus: Results of radio occultation measurements with Voyager, *J. Geophys. Res.*, *92*(A13), 14,987–15,001.

Lukin, D. S., and E. A. Palkin (1982), The numerical canonical method for solution of the diffraction problems of the electromagnetic waves propagation in inhomogeneous media, Moscow Phys. Tech. Inst., Moscow.

Marouf, E. A., and G. L. Tyler (1982), Microwave edge diffraction by features in Saturn's rings: Observations with Voyager 1, *Science*, *217*, 243–245.

Miller, M. A., and E. V. Suvorov (1992), *Maxwell's Equations*, *Phys. Encycl.*, vol. 3 (in Russian), Big Russ. Encycl., Moscow.

Müller, C. (1969), *Foundations of the Mathematical Theory of Electromagnetic Waves*, Springer-Verlag, New York.

Pavelyev, A. (1998), On the possibility of radio holographic investigation on communication link satellite-to-satellite, *J. Commun. Technol. Electron.*, *43*(8), 126–131.

Pavelyev, A., and A. I. Kucherjavenkov (1978), Refraction attenuation in the planetary atmospheres, *Radio Eng. Electron. Phys.*, *23*(7), 13–19.

Pavelyev, A., and S. D. Yeliseyev (1989), Study of the atmospheric layer near the ground using bistatic radar, *J. Commun. Technol. Electron.*, *34*(9), 124–130.

Pavelyev, A., A. V. Volkov, A. I. Zakharov, S. A. Krytikh, and A. I. Kucherjavenkov (1996), Bistatic radar as a tool for Earth investigation using small satellites, *Acta Astronaut.*, *39*, 721–730.

Pavelyev, A., A. I. Zakharov, A. I. Kucherjavenkov, E. P. Molotov, A. I. Sidorenko, I. L. Kucherjavenkova, and D. A. Pavelyev (1997), Propagation of radio waves reflected from Earth's surface at grazing angles between a low-orbit space station and geostationary satellite, *J. Commun. Technol. Electron.*, *42*(1), 45–50.

Pavelyev, A., et al. (2002a), First application of the radio holographic method to wave observations in the upper atmosphere, *Radio Sci.*, *37*(3), 1043, doi:10.1029/2000RS002501.

Pavelyev, A., Y. A. Liou, C. Y. Huang, C. Reigber, J. Wickert, K. Igarashi, and K. Hocke (2002b), Radio holographic method for the study of the ionosphere, atmosphere and terrestrial surface from space using GPS occultation signals, *GPS Solutions*, *6*, 101–108.

Stratton, J. W. (1941), *Electromagnetic Theory*, 616 pp., McGraw-Hill, New York.

Ström, S. (1991), Introduction to integral representation and integral equations for time-harmonic acoustic, electromagnetic and elastodynamic wave fields, in *A Series of Handbooks on Mechanics and Numerical Methods, Third Series: Acoustic, Electromagnetic, and Elastic Wave Scattering*, vol. 1, *Field Representations and Introduction to Scattering*, edited by V. V. Varadan, A. Lakhtakia, and V. K. Varadan, chap. 2, pp. 37–141, Elsevier Sci., New York.

Vladimirov, V. S. (1971), *Equations of Mathematical Physics*, Marcel Dekker, New York.

Wehner, D. R. (1987), *High Resolution Radar*, Ed. Artech House, Norwood, Mass.

Zeldovich, B. Y., N. F. Pilipeckii, and V. V. Shkunov (1985), *Inversion of the Wave Fronts* (in Russian), Nauka, Moscow.

Zverev, V. A. (1975), *Radio-optics*, Soviet Radio, Moscow.

Y. A. Liou, Centre for Space and Remote Sensing Research, National Central University, Jung-Li, 320, Taiwan. (yueian@csrsr.ncu.edu.tw)

A. G. Pavelyev, Institute of Radio Engineering and Electronics, Russian Academy of Sciences, Fryazino, Vvedenskogo sq. 1, 141191 Moscow, Russia. (pvlv@ms.ire.rssi.ru)

J. Wickert, GeoForschungsZentrum Potsdam, Telegrafenberg, D-14473 Potsdam, Germany. (wickert@gfz-potsdam.de)